AD-A243 861

Final Report

DTIC
ELECTE
DEC 2 4 1991
S D
C

on

AFOSR-TR- 91 0000

HIGH-POWER MICROWAVE BREAKDOWN OF DIELECTRIC INTERFACES

November 15, 1991

Air Force Office of Scientific Research
Grant No. 88-0102

PULSED POWER LABORATORY
DEPARTMENT OF ELECTRICAL ENGINEERING
TEXAS TECH UNIVERSITY
LUBBOCK, TEXAS 79409-3102

91-18898

Approved for public release;
Distribution Unlimited

"The views and conclusions contained in this document are those of the authors and should not be interpreted as necessarily representing the official policies or endorsements, either expressed or implied, of the Department of the Air Force of the United States Government."

REPORT DOCUMENTATION PAGE

Form Approved
OMB No. 0704-0188

Public reporting burden for this collection of information is estimated to average 1 hour per response, including the time for reviewing instructions, searching existing data sources, gathering and maintaining the data needed, and completing and reviewing the collection of information. Send comments regarding this burden estimate or any other aspect of this collection of information, including suggestions for reducing this burden, to Washington Headquarters Services, Directorate for Information Operations and Reports, 1215 Jefferson Davis Highway, Suite 1204, Arlington, VA 22202-4302, and to the Office of Management and Budget, Paperwork Reduction Project (0704-0188), Washington, DC 20503

1. AGENCY USE ONLY (Leave blank)	2. REPORT DATE	3. REPORT TYPE AND DATES COVERED
	11 November 1991	FINAL, 15 January 1988 to 14 April 1991

4. TITLE AND SUBTITLE
High Power Microwave Breakdown of Dielectric Interfaces

5. FUNDING NUMBERS
2301/A7

6. AUTHOR(S)
M. Kristiansen, L. Hatfield, Mark Crawford, and Steve Calico

7. PERFORMING ORGANIZATION NAME(S) AND ADDRESS(ES)
Texas Tech University
Department of Electrical Engineering
P.O. Box 43102
Lubbock, TX 79409

8. PERFORMING ORGANIZATION REPORT NUMBER

9. SPONSORING/MONITORING AGENCY NAME(S) AND ADDRESS(ES)
AFOSR/NE
Bldg. 410
Bolling AFB, DC 20332
Barker

10. SPONSORING/MONITORING AGENCY REPORT NUMBER
AFOSR-88-0102

11. SUPPLEMENTARY NOTES

12a. DISTRIBUTION/AVAILABILITY STATEMENT
Approved for public release; distribution unlimited.

12b. DISTRIBUTION CODE

13. ABSTRACT *(Maximum 200 words)*

The goal of this project is the study of the electrical breakdown, due to microwaves, which occurs on the surface of vacuum/atmosphere interfaces. This is a final report for AFOSR Grant No. 88-0102, that began in January, 1988. This report, however, will concentrate on the results since the last annual report, dated September 3, 1990.

In the past year, the system was fired over 300 times while investigating the breakdown process. Window materials, coatings, surface textures, shapes, and ambient gases were all varied and the results recorded. The diagnostics system was timed to provide temporal correlation between the different signals. Using the particle-in-cell code (MAGIC), overall microwave power and field information has been calculated for the various window configurations.

The bulk of these shots were taken using about one-half of the available power from the machine. Recently, the machine was fired several times at near maximum values. Weak points in the machine design were discovered and corrected. Research is continuing, under AFOSR grant No. 91-0260, using the higher power levels from the machine.

14. SUBJECT TERMS	15. NUMBER OF PAGES
Microwaves, Window-Breakdown, Surface-Flashover, Radio-Frequency	32
	16. PRICE CODE

17. SECURITY CLASSIFICATION OF REPORT	18. SECURITY CLASSIFICATION OF THIS PAGE	19. SECURITY CLASSIFICATION OF ABSTRACT	20. LIMITATION OF ABSTRACT
Unclassified	Unclassified	Unclassified	

Summary

The goal of this project is the study of the electrical breakdown, due to microwaves, which occurs on the surface of vacuum/atmosphere interfaces. This is a final report for AFOSR Grant No. 88-0102, that began in January, 1988. This report, however, will concentrate on the results since the last annual report dated September 3, 1990.

In the past year, the system was fired over 300 times while investigating the breakdown process. Window materials, coatings, surface textures, shapes, and ambient gases were all varied and the results recorded. The diagnostics system was timed to provide temporal correlation between the different signals. Using the particle-in-cell code (MAGIC), overall microwave power and field information has been calculated for the various window configurations.

The bulk of these shots were taken using about one-half of the available power from the machine. Recently, the machine was fired several times at near maximum values. Weak points in the machine design were discovered and corrected. Research is continuing, under AFOSR grant No. 91-0260, using the higher power levels from the machine.

DTIC COPY INSPECTED

Accession For
NTIS GRA&I
DTIC Tab
Unannounced
Justification
By
Distribution/
Availability Codes
Dist | Avail and/or special
A-1

Project Overview

The electrical breakdown of a dielectric window in the atmosphere due to a high power microwave pulse has been investigated. Electrical breakdown of the window creates a plasma, through which the microwaves cannot propagate or are attenuated and/or refracted. Several factors have been studied, including the effects of different window materials, window shapes, window coatings and ambient gases. If the breakdown strength of the window can be improved, the microwave power through the window can be increased.

The high-power microwaves are produced by a virtual cathode oscillator (vircator)[1]. An overall schematic drawing of the project is shown in Figure 1. An electron beam is injected into a waveguide where the space-charge limit is exceeded, a virtual cathode that oscillates in space and time is formed, and the microwaves are extracted. The experiment consists of a 10 Ω, 12.5 ns one-way transit time, coaxial pulse-forming line (PFL) that is charged from a Marx bank and switched into the vacuum diode through a self breaking spark gap. The Marx tank, PFL, and output switch are all filled with transformer oil. The vacuum diode and the waveguide are evacuated with a diffusion pump and two mechanical roughing pumps. The best vacuum attained to date has been better than 2×10^{-6} Torr. The end of the waveguide where the window is located is contained in an anechoic chamber which provides a reflection-free environment in which to observe the breakdown.

The diagnostics system is able to directly measure the Marx bank voltage, diode current, diode voltage, microwave power density at a given location in the radiation pattern, and the temporal variations in the light from the breakdown. In addition, two mechanical cameras are placed to capture time-integrated photographs from inside the anechoic chamber. One camera views the window and captures the breakdown image, the other photographs the radiation pattern as detected by an array of fluorescent tubes placed at the end of the anechoic chamber.

In addition to the actual experimental equipment, a great deal of research has been done using the simulation code MAGIC[2]. MAGIC is a two-and-one-half dimensional, fully relativistic, particle-in-cell code. Using various university computing facilities, a number of simulations have been run to investigate the operation of the vircator and waveguide window.

Research Results

Over the duration of the high-power microwave research, the machine has been fired over 380 times. Most of these shots were taken while various parameters affecting the window breakdown were varied. A series of different windows were tested on the end of the waveguide. Table 1 gives a summary of the different types of windows which were tested and their designation for reporting purposes.

The first window was a 1" thick Lucite window which was used simply as a blank off plate during the testing phase of the project, this explains why the window numbering begins at two. Each of the windows, except for number 8, is much larger in diameter than the waveguide flange. The larger size allows for ports to be placed in the window for gas filling and venting. The gas is contained by thin, transparent, plastic bags which are taped onto the edge of the window. Plastic tubing is run from the gas supply into the bag through fittings mounted on the outer edge of the window and from the window to a venting pump. The pump provides a quick method of emptying the bag of old gas and refilling it with fresh gas.

The majority of the testing took place at power levels which were capable of breaking down atmospheric air, but not sulfur hexafluoride (SF_6). In addition, even though air broke down, the plasma formed only in the center of the window and did not significantly reduce the propagated microwave power when compared to an SF_6 atmosphere. Figure 2 is a photograph of the microwave breakdown in air.

Because the power level of the machine was not large enough to show a degradation of the microwave power through the window in air, other, electrically weaker gases were used to study the breakdown effects of the various window parameters. This procedure allowed data to be taken without increasing the output of the machine and risking a catastrophic failure in the system. The other gases used were argon and helium. As these gases were used it became obvious that helium is electrically weaker than argon which is weaker than air. All of the data taken for the different window materials, shapes, and surface conditions are taken as relative data for the different gases.

The different materials tested for the window were Lucite, Lexan, and nylon. They were compared to one another as window numbers 2, 3, and 4. Each window was 1/2" thick and tested with the three test gases, air, argon and helium. Figure 3 shows representative photographs of breakdown on all of the planar windows in the various gases. Figures 4, 5, and 6 are propagated microwave power waveforms for Lucite, Lexan, and nylon. respectively. When photographing the breakdown of the windows in

the various gases, the aperture of the camera lens was varied to produce a clear image of the breakdown. In most cases, the f-stop of the camera was set at 8 (larger aperture) for tests in air and at 22 (smaller aperture) for tests in argon and helium. Because of this fact, direct comparisons of the photographs can be misleading but, in general, the breakdown of helium was brighter than argon which was substantially brighter than air. By reviewing the data from the tests done on the three different window materials, it can be seen that the choice between Lucite, Lexan, or nylon has very little influence on the breakdown of the microwave window. The rest of the tests were conducted using whichever material was best suited for the particular test parameters.

Windows 5 and 6 each had a region of the window center painted with Aquadag (graphite in an aqueous solution). These windows were tried to test a theory about the mechanism of the breakdown. It was believed that the secondary electrons generated from the window surface were strongly influencing the breakdown. The Aquadag has a low secondary electron emission coefficient and was supposed to decrease the amount of secondaries provided by the window. Window 5 had a 2" diameter disk of Aquadag painted in the center. The layer of Aquadag was applied with a paintbrush and was relatively thick. When window 5 was tested, the breakdown in air did seem to decrease somewhat, but the photographic evidence of plasma formation in argon and helium was inconclusive. The size of the Aquadag patch was increased to an 8" diameter because it was believed that not enough of the window had been covered to affect the breakdown in the lower threshold gases argon and helium. The eight inch patch on window 6 effectively covers the entire waveguide aperture. When window 6 was tested, almost no microwave power was able to penetrate into the anechoic chamber. The Aquadag layer absorbed or reflected nearly all of the microwave power. The relatively thick Aquadag layer does not provide any benefit to microwave transmission. It is possible, however, that a very thin (e.g. vacuum vapor deposited) layer of carbon may show some benefit.

It has been shown that the unipolar, pulsed surface voltage hold-off strength of Lexan in vacuum can be affected by up to a factor of two by randomly roughening the surface with different grit sandpapers[3]. The largest improvement was attained when 1200 grit sandpaper was used. Windows 7 and 9 were 1/2" thick, planar Lexan with the atmosphere side of the window randomly roughened. Twelve hundred grit was used on window 7 and, for comparison, window 9 was sanded with 80 grit.

Because of the availability of planar windows already constructed at this stage of the experiment, a set of tests were conducted to see what effect the relative humidity in air has on the power propagating through the region close to the window. What is designated as window 12 is actually window 3 with humidified air on the atmospheric

side of the window. Atmospheric air was bubbled through water, then pumped into the plastic bag enclosing the window. Measurements with a hygrometer indicated that relative humidities of 76% (12a) and 83% (12b) were obtained. When tested, these humidified windows had no effect on the propagated microwave power. Except in the case of the windows coated with Aquadag, no changes made to planar windows had any dramatic effect on the microwave propagation.

At this point, a series of non-planar windows were tested. The first window, designated window 8, was a one-inch thick Lucite window onto which a cone was cemented. The cone was two inches in diameter at the base and was cut to a 45° angle. When this window was tested, the glue joint between the window and the cone consistently broke down as shown in Figure 7. Subsequent non-planar windows were constructed from single pieces of Lexan.

The 45° angle was chosen because of its use in pulsed vacuum insulator technologies. Two more windows were constructed, each from a 2" thick Lexan blank. The first, used for windows 10 and 14, was machined to have a protruding 45° cone, 3" in diameter in the center of the window with the bulk of the window being 1/2" thick. The second, used for windows 11 and 13, was machined to have an inverted 45° cone, 3" in diameter cut into the center of the window with the bulk of the window being 2" thick. The separate designations for each window indicates in which direction the window was facing. Window 10 is the protruding cone with the cone placed in the atmosphere while window 14 has the cone in the vacuum. Similarly, window 11 is the inverted cone with the cone on the atmospheric side and window 13 has the cone in the vacuum.

Results from the four one-piece non-planar windows are in the form of photographs of the breakdown and comparisons of the waveforms for each of the test gases. Window 10 (protruding cone in atmosphere) results are shown in Figures 8 and 9, window 11 (inverted cone in atmosphere) results are shown in Figures 10 and 11, window 13 (inverted cone in vacuum) results are shown in Figures 12 and 13, and window 14 (protruding cone in vacuum) results are shown in Figures 14 and 15.

Some information from the data taken on the four non-planar windows can be seen directly. Most notably there is no breakdown in air and much less breakdown in argon for the inverted cone in atmosphere when compared to the other windows. Because of the qualitative nature of the photographs, it is not possible to draw conclusions about the breakdown in helium compared to that for the planar and protruding cone windows. It can be seen that the threshold for breakdown is barely exceeded on window 13 (inverted cone in vacuum), hence the small plasma volume,

while on window 14 (protruding cone in vacuum) there is a substantial breakdown volume.

For the non-planar windows oriented with the structure of the window facing into the anechoic chamber (windows 10 and 11) the protruding cone shows generally good performance in all gases while the inverted cone shows enhanced performance only in argon. When the windows are turned around so that the structure is facing into the waveguide the inverted cone performs poorly and the protruding cone shows just average performance in comparison to the other windows.

A more quantitative method for determining the breakdown quantities had to be developed. The shape of the non-planar windows influences the electric and magnetic fields as they propagate through them. Computer simulations using the geometry of the waveguide, window, and anechoic chamber provided a method of determining the fields around and in the window for a given power density detected at the B-dot antenna.

The October, 1990 version of MAGIC provides the ability to put regions of dielectric material into the simulation. Using this property, the waveguide, various windows, and the anechoic chamber containing the B-dot antenna have been simulated very accurately. By comparing the measured values of the magnetic field at the B-dot probe with the magnitude of the waveguide fields required to produce the same magnetic field at a location in the simulation which the matches the physical location of the B-dot antenna, the fields in the waveguide and in and around the window can be calculated. Figures 16 through 25 are field plots of the axial and radial electric fields for a planar window and the four non-planar windows. These plots show contours of constant electric field strength for E_z and E_ρ at a time step corresponding to a maximum of the particular quantity at the window surface. All of the graphs have the same contour level separation (200 kV/m) to facilitate direct comparisons between the different graphs. The solid lines denote regions of positive field strength values and the dashed lines denote regions of negative field strength. The dotted region indicates the dielectric material, and the end of the waveguide can be seen at R=0.1 m.

One interesting conclusion can be drawn from the simulation contour plots. The breakdown field for Lexan in air can be determined by comparing the maximum axial electric field for the planar window (window 3) and the inverted cone in atmosphere (window 11). The maximum field on the planar window is 2.2 MV/m while the maximum field on the inverted cone window is 1.8 MV/m. In experimentation, a plasma forms on the planar window but does not form on the inverted cone window. This leads to the conclusion that the pulsed microwave breakdown strength of Lexan in air is

between 1.8 MV/m and 2.2 MV/m. Breakdown strengths cannot be inferred for the other gases because there is always breakdown in them.

In order for a comparison to be made between different windows, an unbiased method of comparison must be formulated. One easy way to do this would be to subject each window to an identical microwave pulse and measure the transmitted power. There are no provisions to measure the microwave power in the waveguide on this experiment, so an alternate technique must be used to determine the repeatability of the incident pulse. It is known that the diode voltage and diode current are very repetitive from shot to shot, varying only in magnitude. Multiplying the diode voltage by the diode current gives the beam power, which can then be integrated with respect to time to give the beam energy. If it is assumed that the physics of the microwave generation in the vircator is predictable and well behaved, the repeatability of the beam energy suggests repeatability of the generated microwave radiation. The results of these calculations are shown in Figure 26 . It can be seen that the last five windows of interest were tested under very similar conditions but the first four show some variances. Windows 5 and 6 (the windows with Aquadag painted in the center) and window 8 (the two-piece non planar window) and windows 12a and 12b (the humidified windows) have not been included in these calculations due to poor performance or lack of different gases tested with these windows.

If the microwave power is integrated in time one gets the energy in the microwave pulse. This is the microwave energy that is propagated into the anechoic chamber. The ratio of the microwave energy to the beam energy yields a device efficiency, where the device is comprised of the vircator and the window. If the vircator is assumed to behave repeatably then this ratio can be interpreted as a measure of the relative efficiency of the different windows. This method should also reduce the effect of beam energy variations demonstrated in Figure 26. A graph showing these calculated device efficiencies is shown in Figure 27. When comparing window performances, it must be realized that there is another determining factor in the window performance, besides the reflection or absorption of microwaves by the breakdown plasma. In general, two windows of identical geometry but different dielectric constant will have different reflection coefficients. Therefore, the material of the window, as well as the shape, must be kept in mind when making these comparisons.

In summary, the Lexan window roughened with 1200 grit sandpaper gave superior performance when compared to almost any other window in any gas, while the Lexan window roughened with 80 grit sandpaper gave inferior performance. The best performance in air was by the protruding cone in atmosphere. This is attributed to the

fact that the breakdown plasma takes place on the end of the cone which is further into the radiation pattern and blocks less of the aperture. The inverted cone in atmosphere gave the best performance in argon. This is probably because the poor transmission of the thicker window limits the electric field strength to a value below the breakdown threshold in argon for more of the area of the window. Since the threshold for breakdown is not exceeded over more of the aperture, more power is allowed to propagate. The best window in helium was the planar Lexan window roughened with 1200 grit sandpaper.

Work on the breakdown studies is continuing under a new contract. A thin inverted cone window has been constructed which, it is hoped, will provide the low axial electric fields of window 11 without the losses from the thickness. A window with the thin vacuum deposited carbon layers will be manufactured and tested. Also, a matching stub is being designed which will provide destructive interference at the window surface in an attempt to lower the electric fields These methods. as well as several others are presently under study.

Publications

Three papers were written for publication about aspects of the research:

S. Calico, M. Crawford, M. Kristiansen, and H. Krompholz, "The design and calibration of a very fast current probe for the measurement of short pulses" *Rev. Sci. Instrum.* 62 (6), June 1991

Crawford, S. Calico, M. Kristiansen, and H. Krompholz "Pulsed Vacuum Diode Diagnostics at the Texas Tech University High-Power Microwave Facility" presented in poster form and published in the proceedings of the 8th International Pulsed Power Conference in San Diego, California, June 1991

Crawford, S. Calico, M. Kristiansen, and L. Hatfield, "Pulsed Microwave Breakdown of Solid Dielectric/Gas Interfaces", presented in poster form and published in the proceedings of the 20th International Conference on the Phenomenon in Ionized Gases (ICPIG XX) in Barga, Italy, July 1991.

Personnel

Principal Investigators: Dr. M. Kristiansen, C. B. Thornton/P. W. Horn Professor of EE and Physics
Dr. L. Hatfield, Professor of Physics

Graduate Students: Steve Calico graduated with his Ph.D in May, 1991 and has gone on to work for the Air Force at Phillips Laboratory.
Mark Crawford earned his Master's in August, 1991 and is continuing his research on the project for his Ph.D.

Interactions

Professor Kristiansen and Mr. Crawford attended the 20th ICPIG in Barga, Italy. Professor Kristiansen presented an invited lecture at the short course presented before the ICPIG.

---

1. V. Grannatstein and I. Alexoff, High Power Microwave Sources. Artech House, Boston, 1987.

2. Bruce Goplen, Larry Ludeking, Gary Warren, and Richard Worl, "Magic User's Manual," Mission Research Corporation Technical Report, MRC/WDC-R-246, October 1990

3. John Drew Smith, Ph.D. Dissertation, Texas Tech University, 1989.

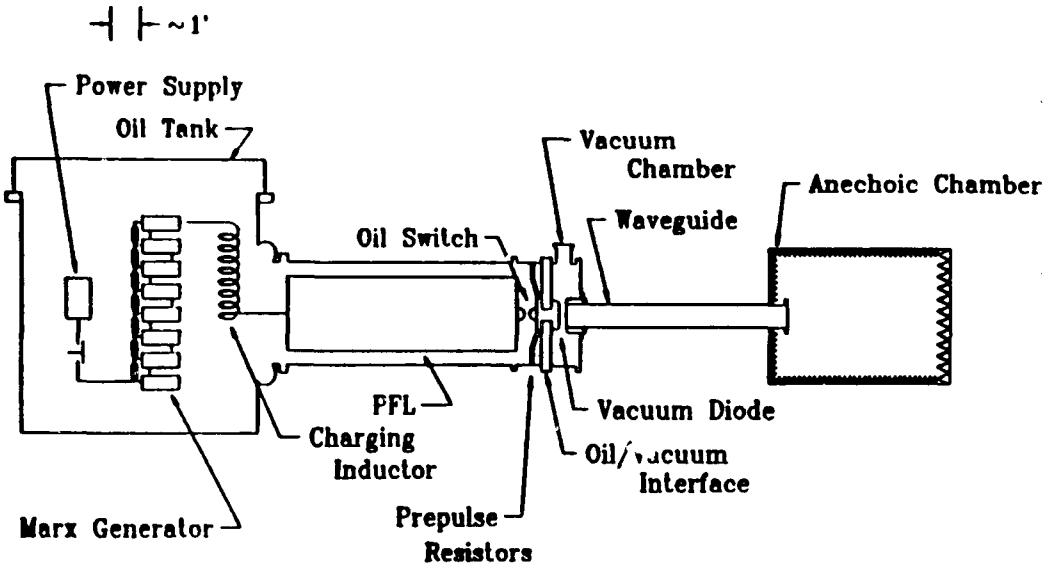

Figure 1. Overall schematic drawing of the experiment.

Table 1. Summary of Windows Tested and Test Conditions

Window Number	Description	Gases Used	Notes	Sketch of Window Shape and Orientation
2	planar Lucite, 1/2" thick, unfaced	Air, Ar, He, SF_6		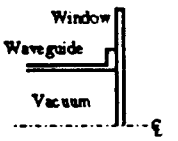
3	planar Lexan, 1/2" thick, unfaced	Air, Ar, He, SF_6		
4	planar nylon, 1/2" thick, faced	Air, Ar, He	black nylon (optically opaque)	

5	planar Lucite, 1/2" thick, unfaced	Air, Ar, He	diameter Aquadag disk painted in the window center	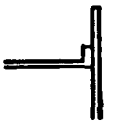
6	planar Lucite, 1/2" thick, unfaced	Air, Ar, He	diameter Aquadag disk painted in the window center	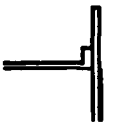
7	planar Lexan, 1/2" thick, faced	Air, Ar, He	random surface roughening with 1200 grit sandpaper	
8	non-planar Lucite, 1" thick, faced	Air, Ar, He	diameter, 45° cone cemented in the window center	
9	planar Lexan, 1/2" thick, faced	Air, Ar, He	random surface roughening with 80 grit sandpaper	
10	non-planar Lexan, 1/2" thick, protruding cone	Air, Ar, He	protruding cone on the atmospheric side	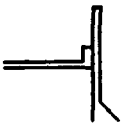
11	non-planar Lexan, 2" thick, inverted cone	Air, Ar, He	inverted cone on the atmospheric side	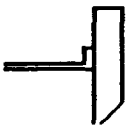
12 a,b	planar Lexan, 1/2" thick, unfaced	Air	and 86%(b) relative humidity	
13	non-planar Lexan, 2" thick, inverted cone	Air, Ar, He	inverted cone on the vacuum side	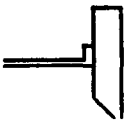

14	non-planar Lexan, 1/2" thick, protruding cone	Air, Ar, He	protruding cone on the vacuum side	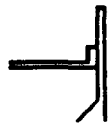

(Air)

Figure 2. Planar window breakdown in air.

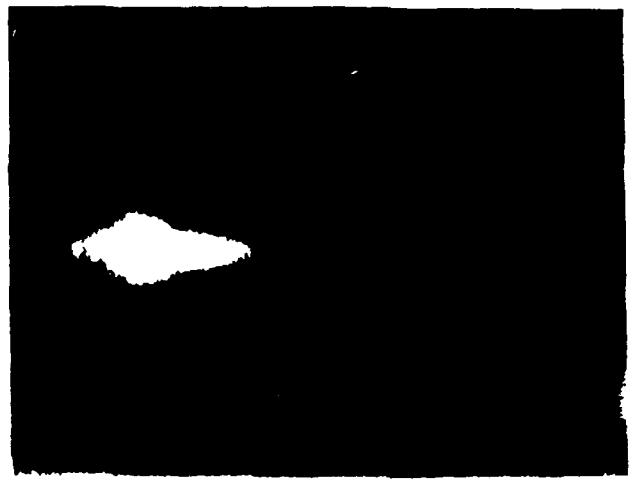

(Air)

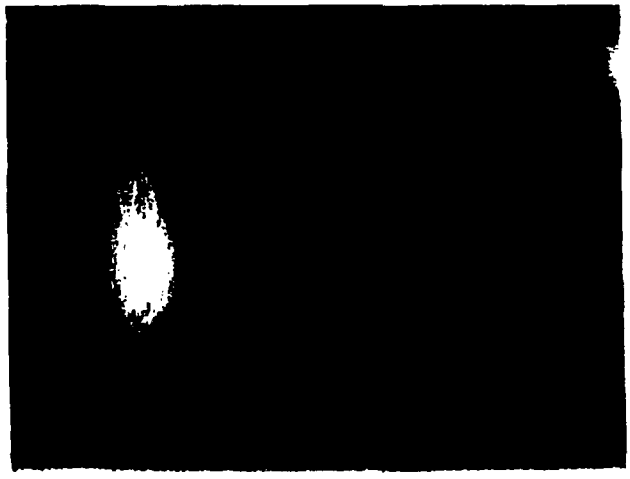

(Ar)

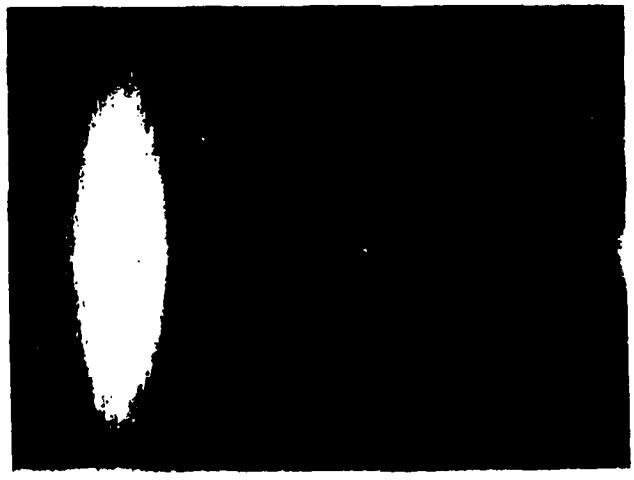

(He)

Figure 3. Representative photographs of breakdown of planar windows.

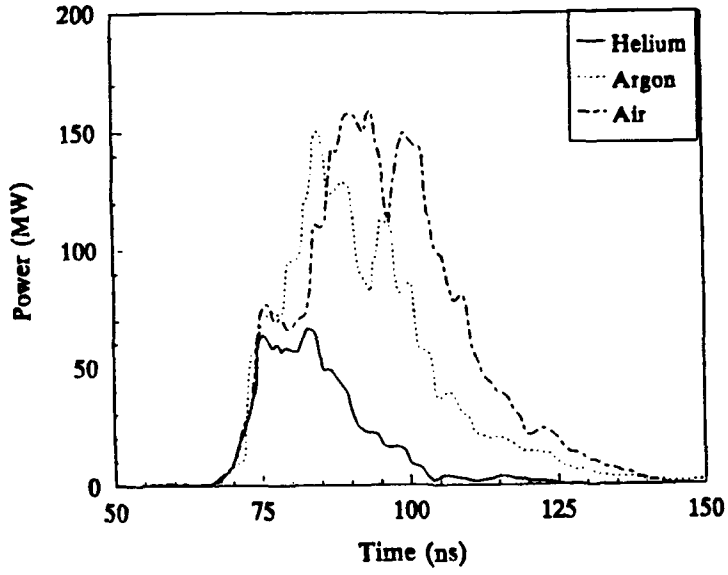

Figure 4. Propagated microwave envelopes in air, argon and helium for planar Lucite, (Window 2).

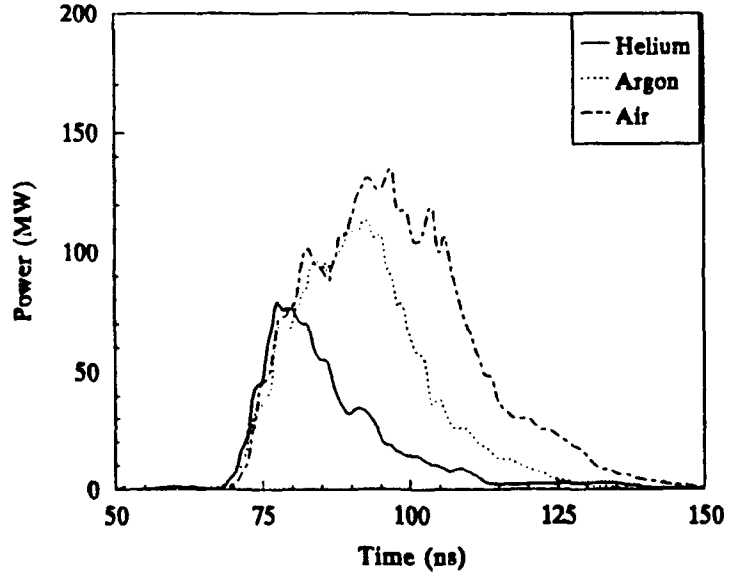

Figure 5. Propagated microwave envelopes in air, argon and helium for planar Lexan, (Window 3).

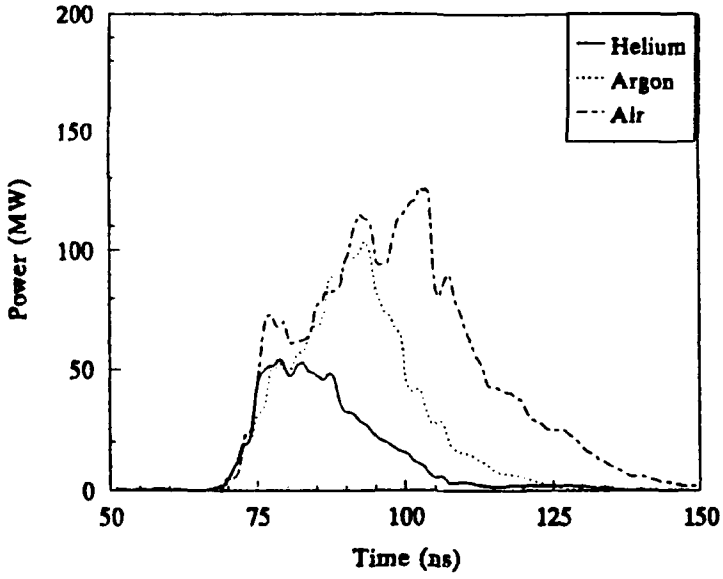

Figure 6. Propagated microwave envelopes in air, argon and helium for black nylon, (Window 4).

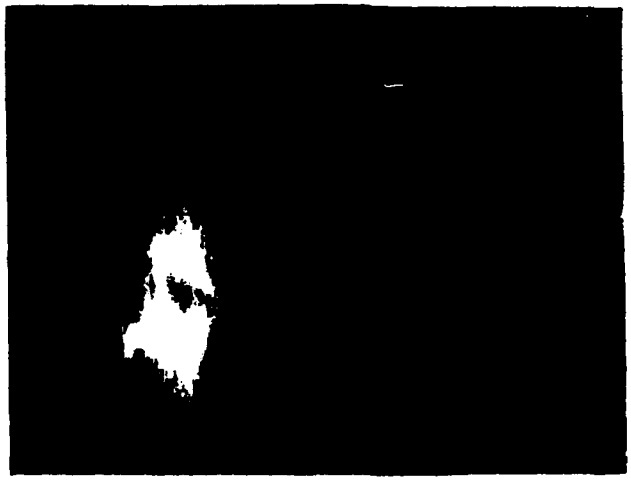

Figure 7. Photograph of window 8 (two-piece non-planar Lucite) breaking down at the glue joint.

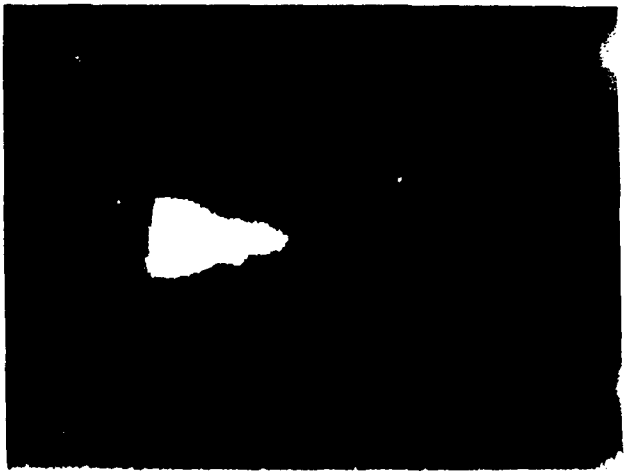

(Air)

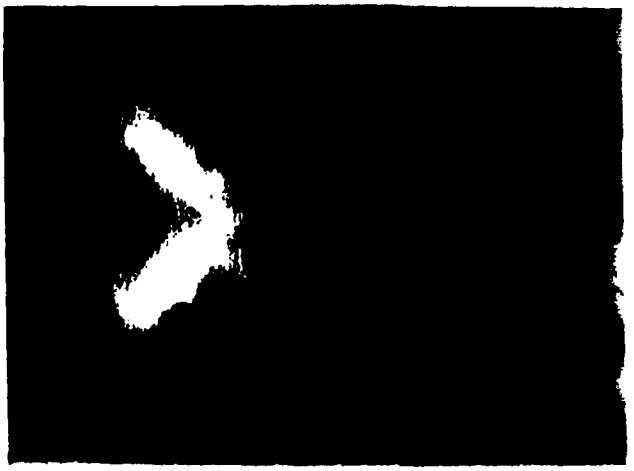

(Ar)

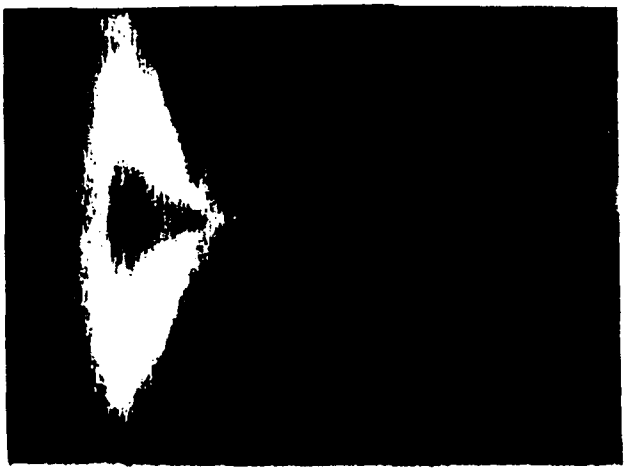

(He)

Figure 8. Photographs of the breakdown in air, argon and helium for protruding cone in atmosphere, (Window 10).

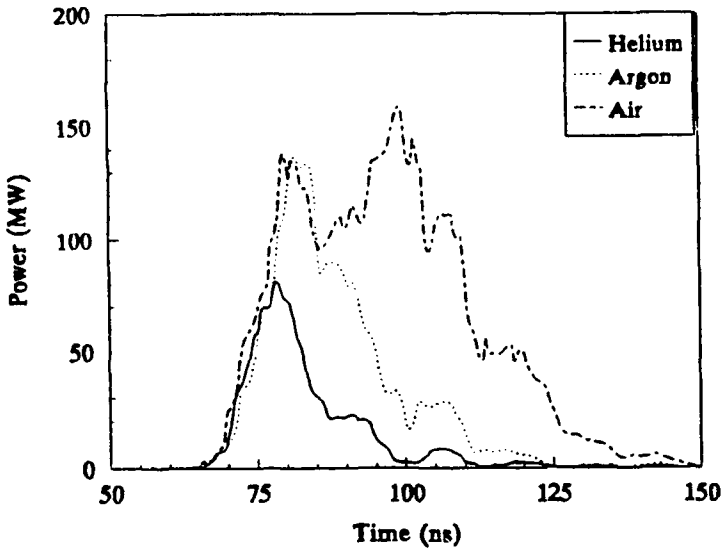

Figure 9. Propagated microwave envelopes in air, argon and helium for protruding cone in atmosphere, (Window 10).

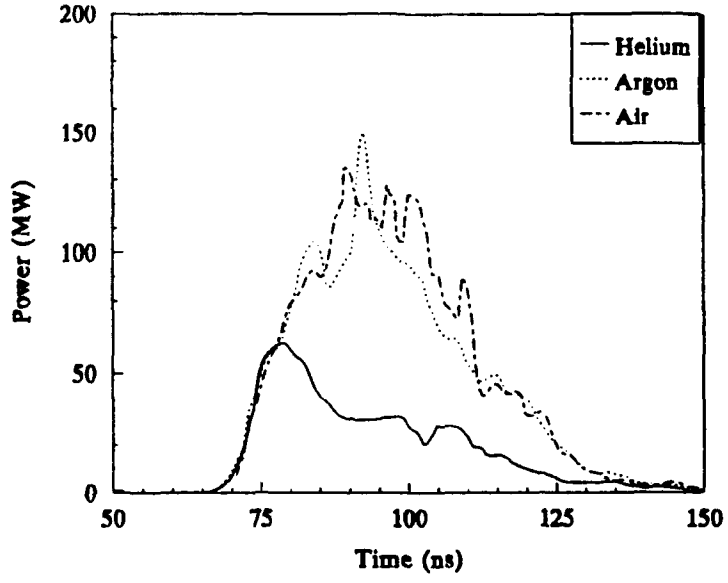

Figure 10. Propagated microwave envelopes in air, argon and helium for inverted cone in atmosphere, (Window 11).

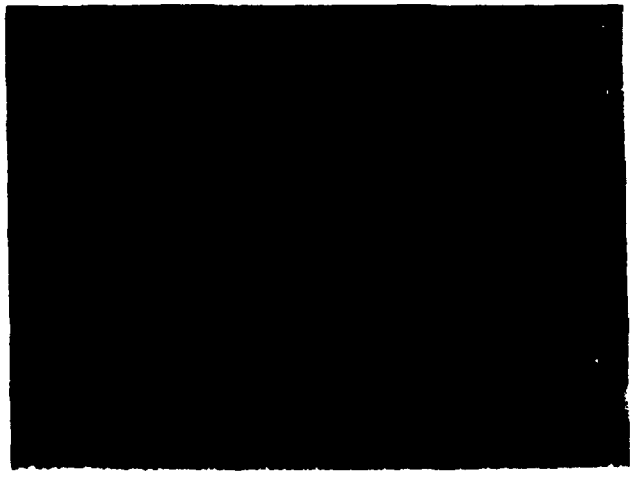

(Air)

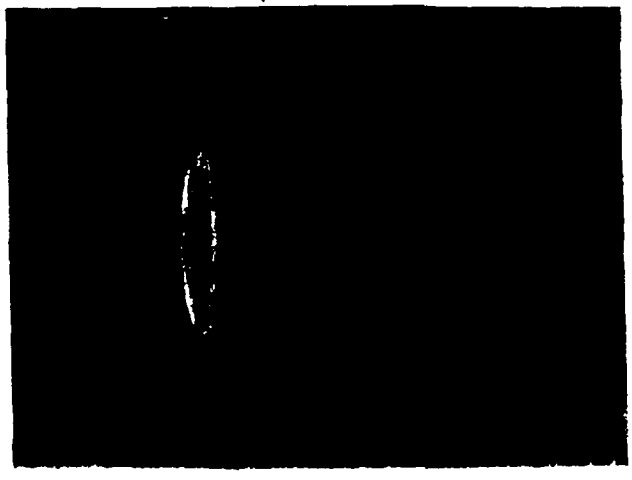

(Ar)

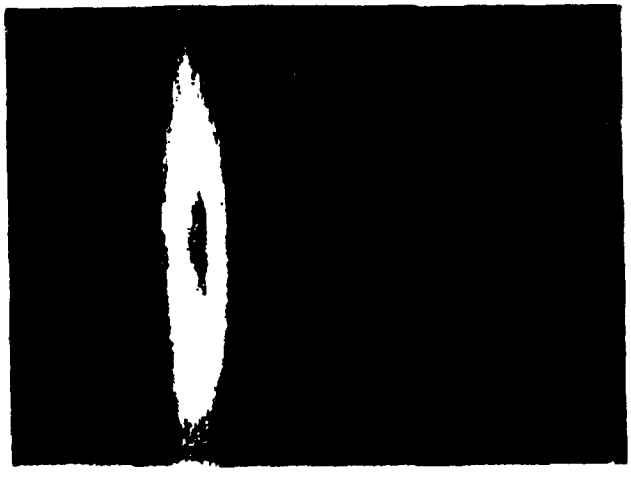

(He)

Figure 11. Photographs of the breakdown in air, argon and helium for inverted cone in atmosphere, (Window 11).

(Air)

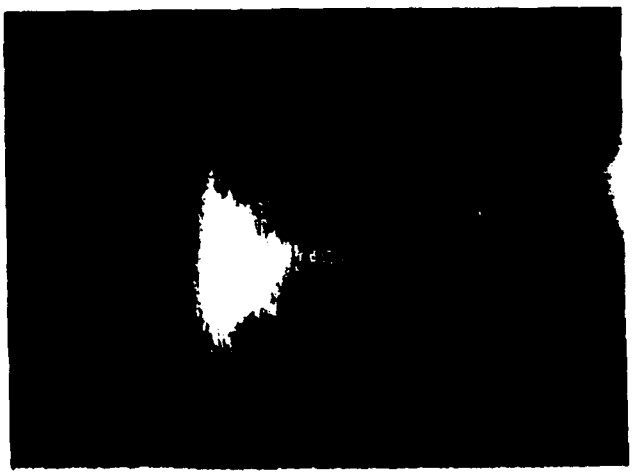

(Ar)

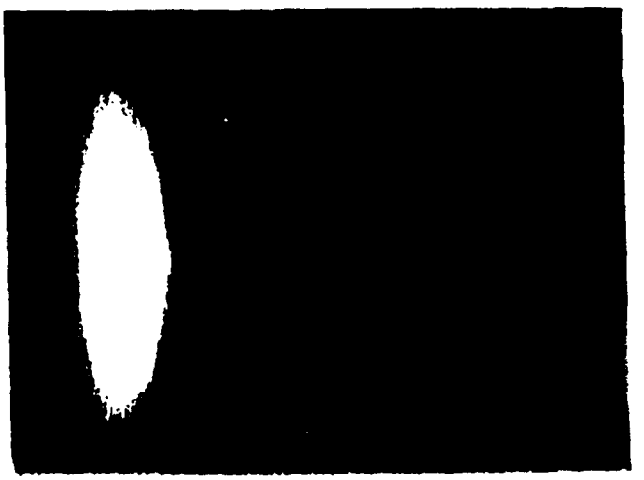

(He)

Figure 12. Photographs of the breakdown in air, argon and helium for inverted cone in vacuum, (Window 13).

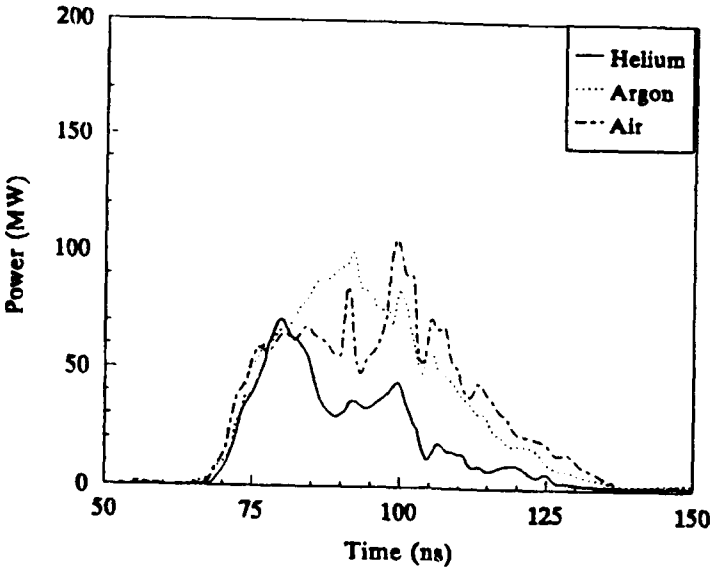

Figure 13. Propagated microwave envelopes in air, argon and helium for inverted cone in vacuum, (Window 13).

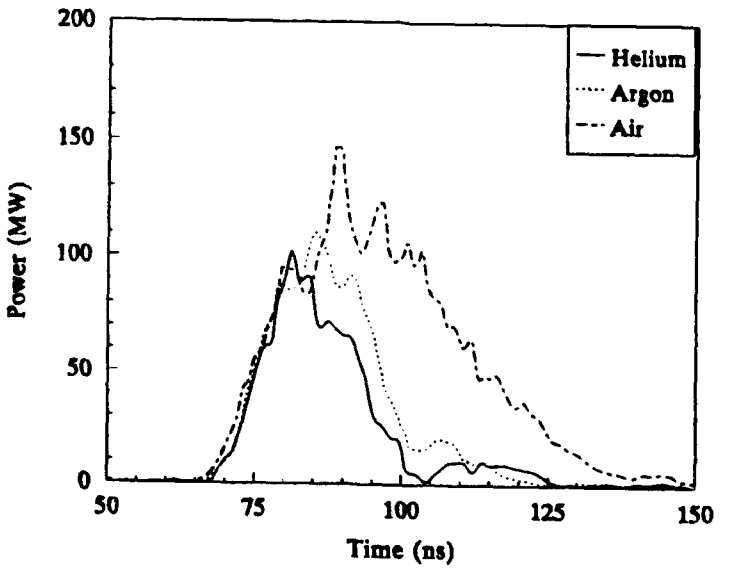

Figure 14. Propagated microwave envelopes in air, argon and helium for protruding cone in vacuum, (Window 14).

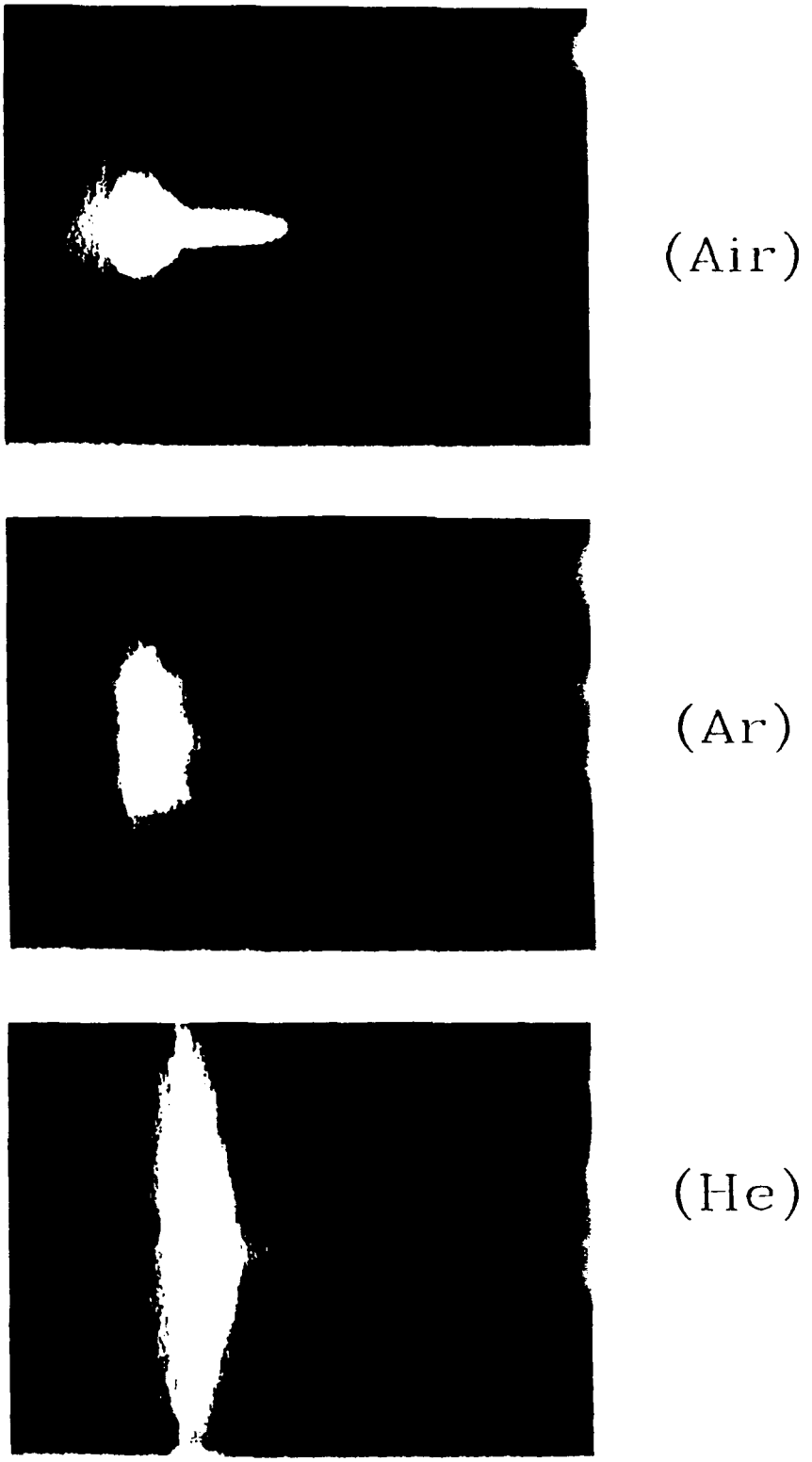

Figure 15. Photographs of the breakdown in air, argon and helium for protruding cone in vacuum, (Window 14).

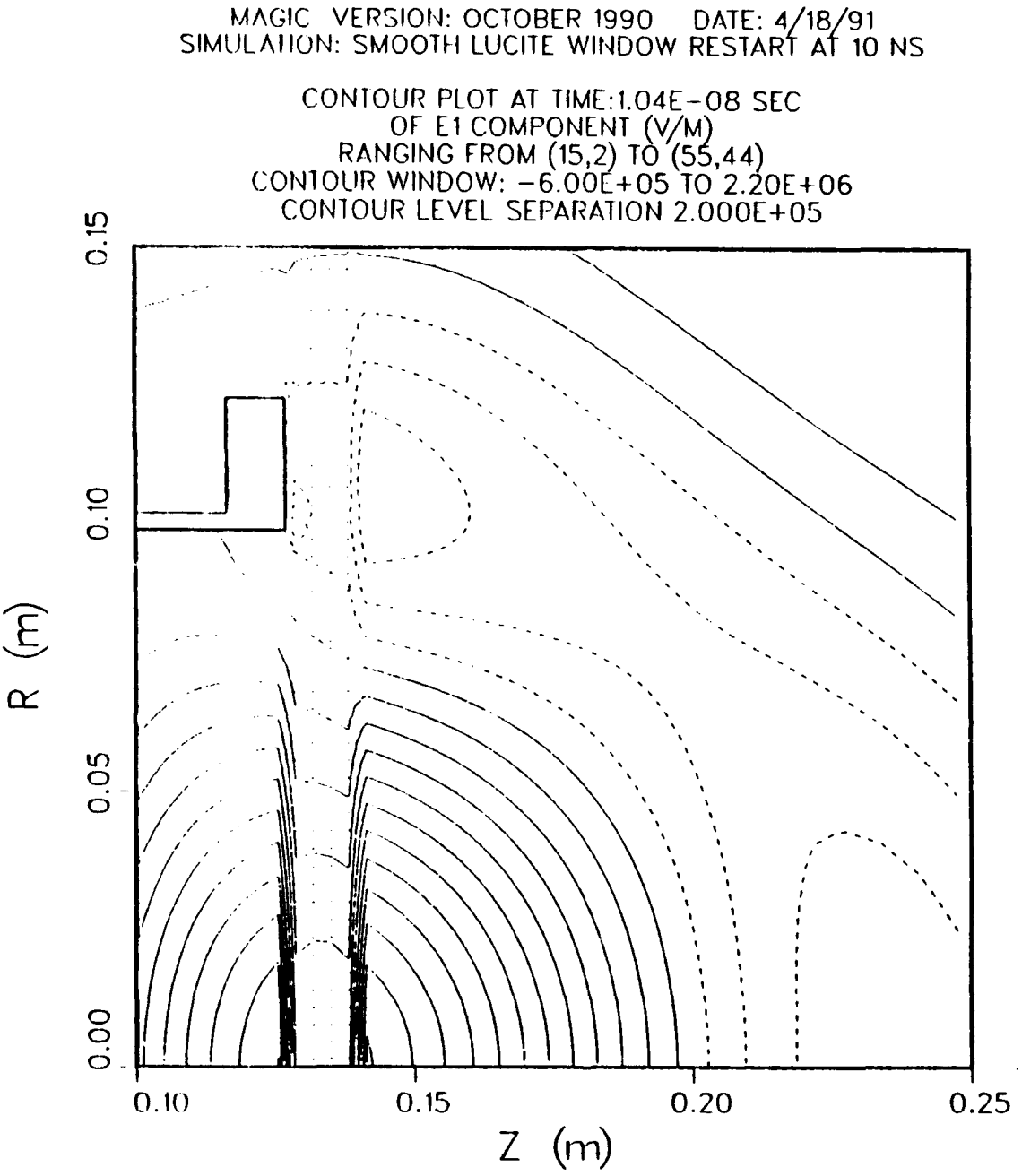

Figure 16. Axial electric field contours for the planar window.

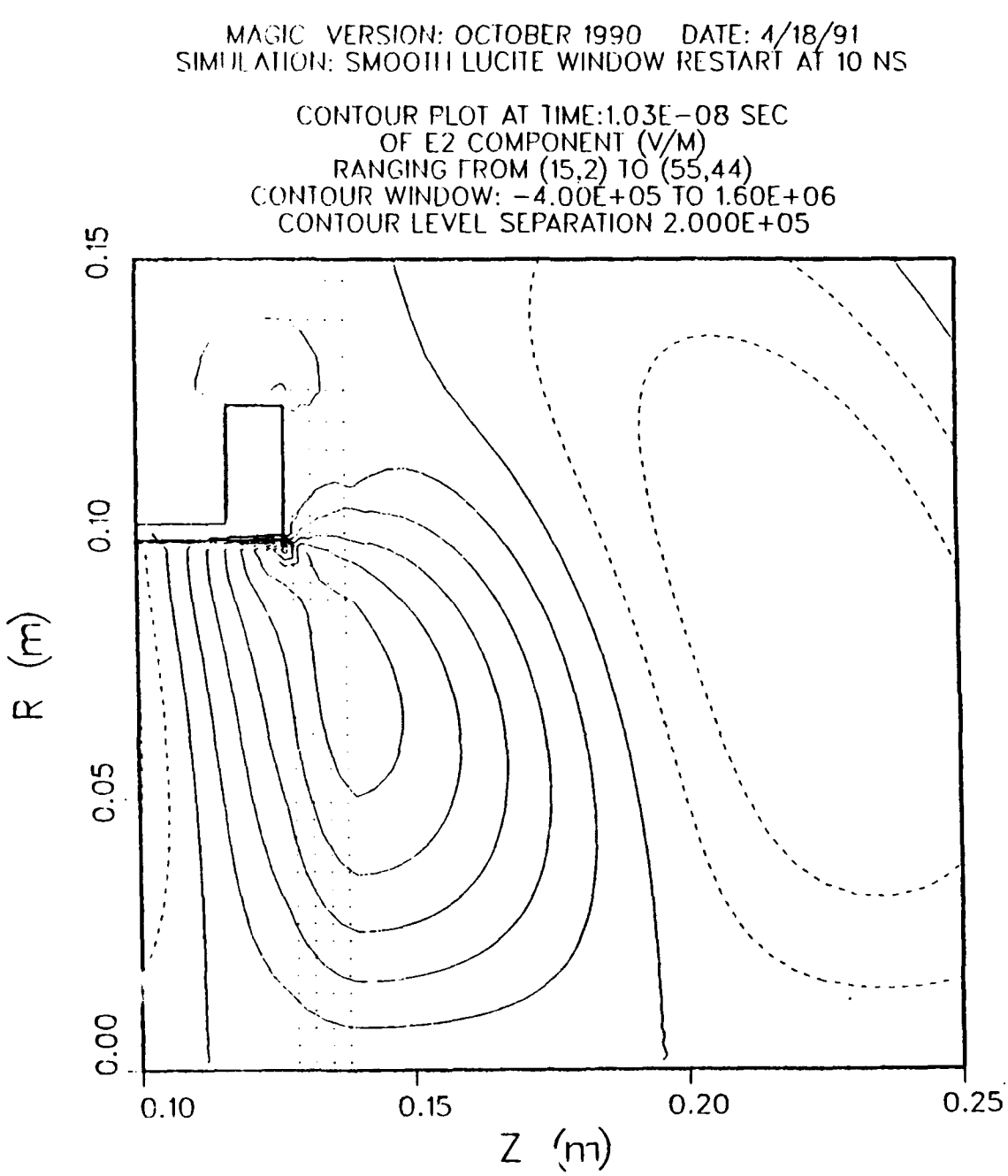

Figure 17. Radial electric field contours for the planar window.

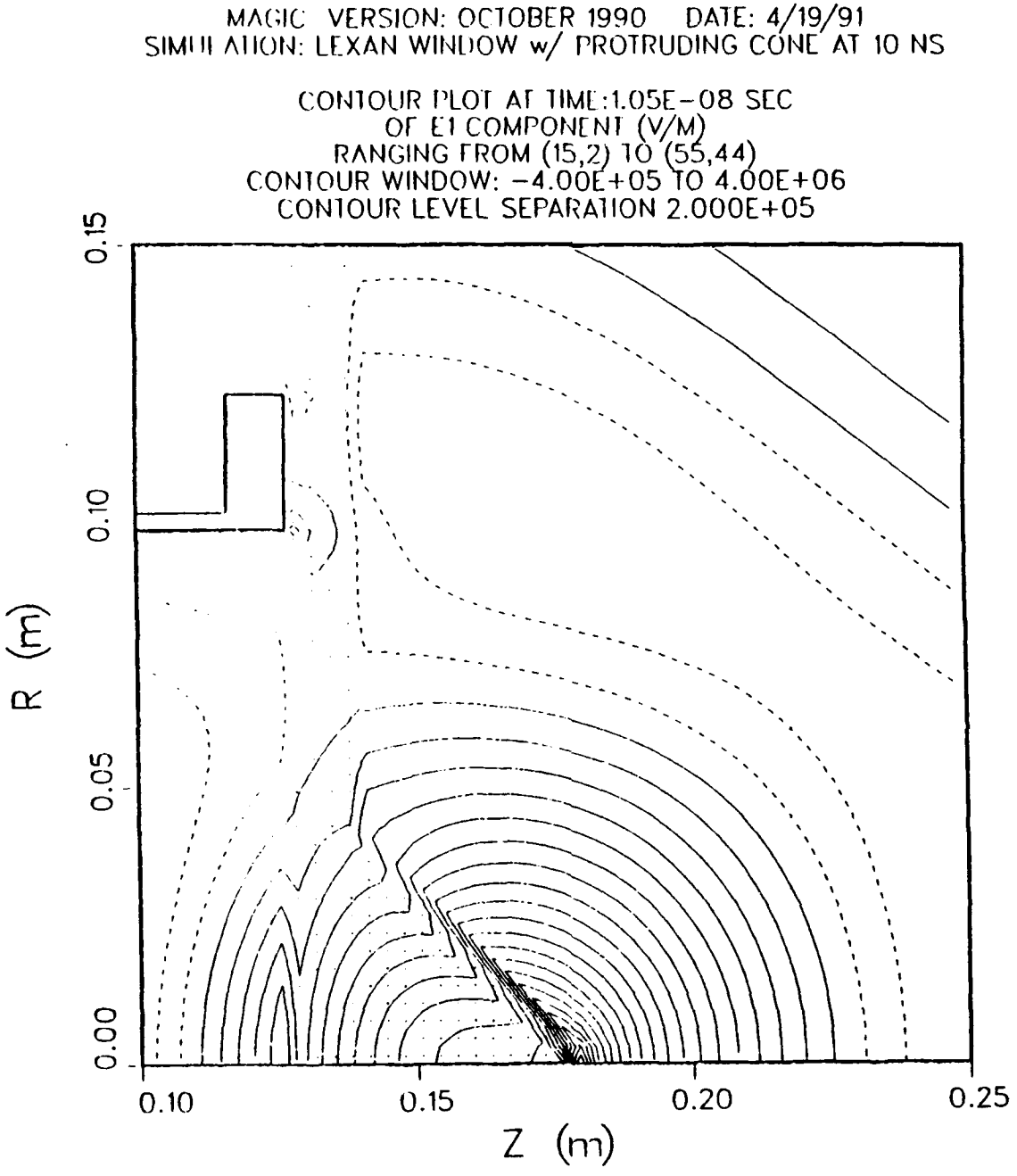

Figure 18. Axial electric field contours for the protruding cone in atmosphere window.

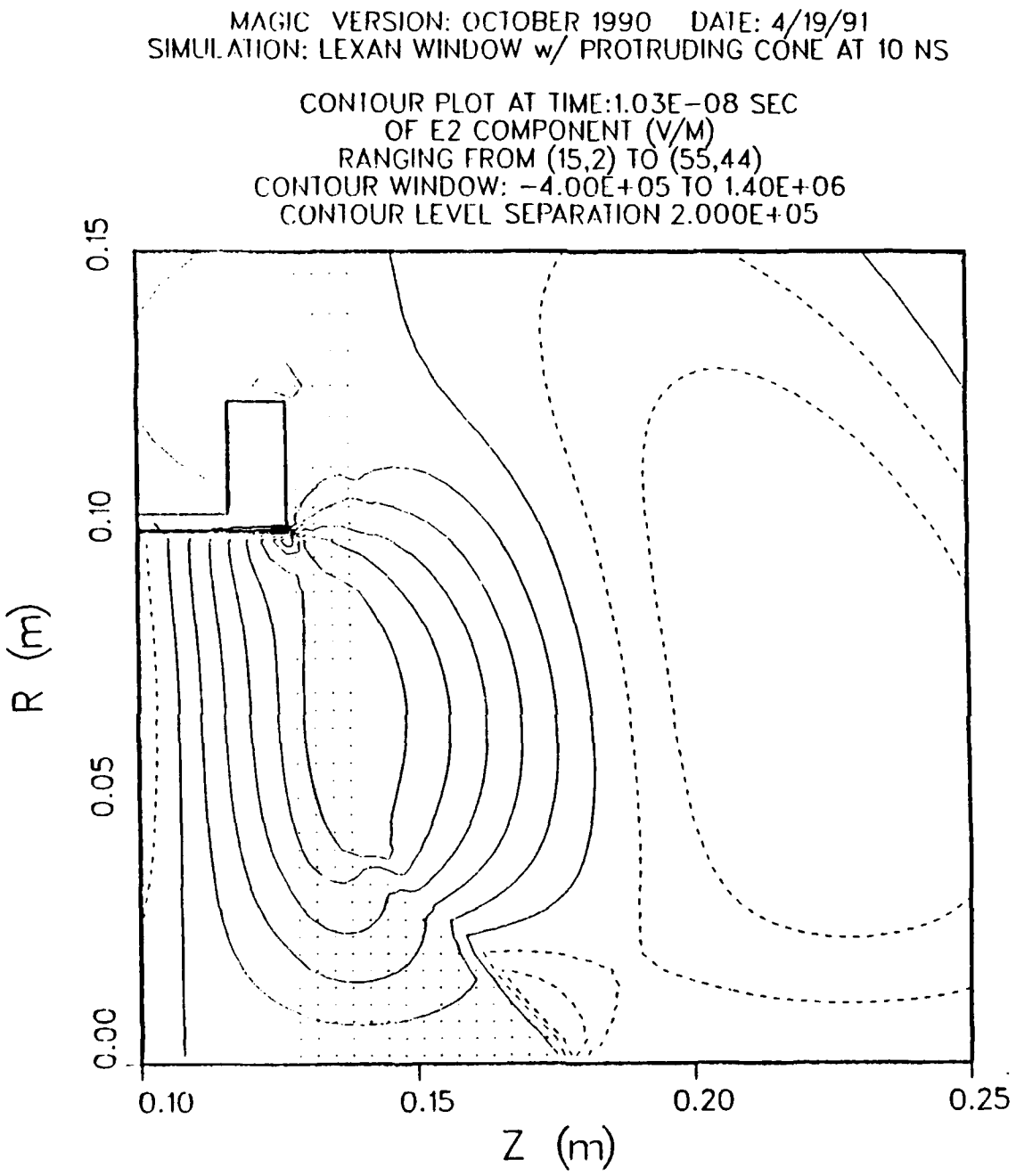

Figure 19. Radial electric field contours for the protruding cone in atmosphere window.

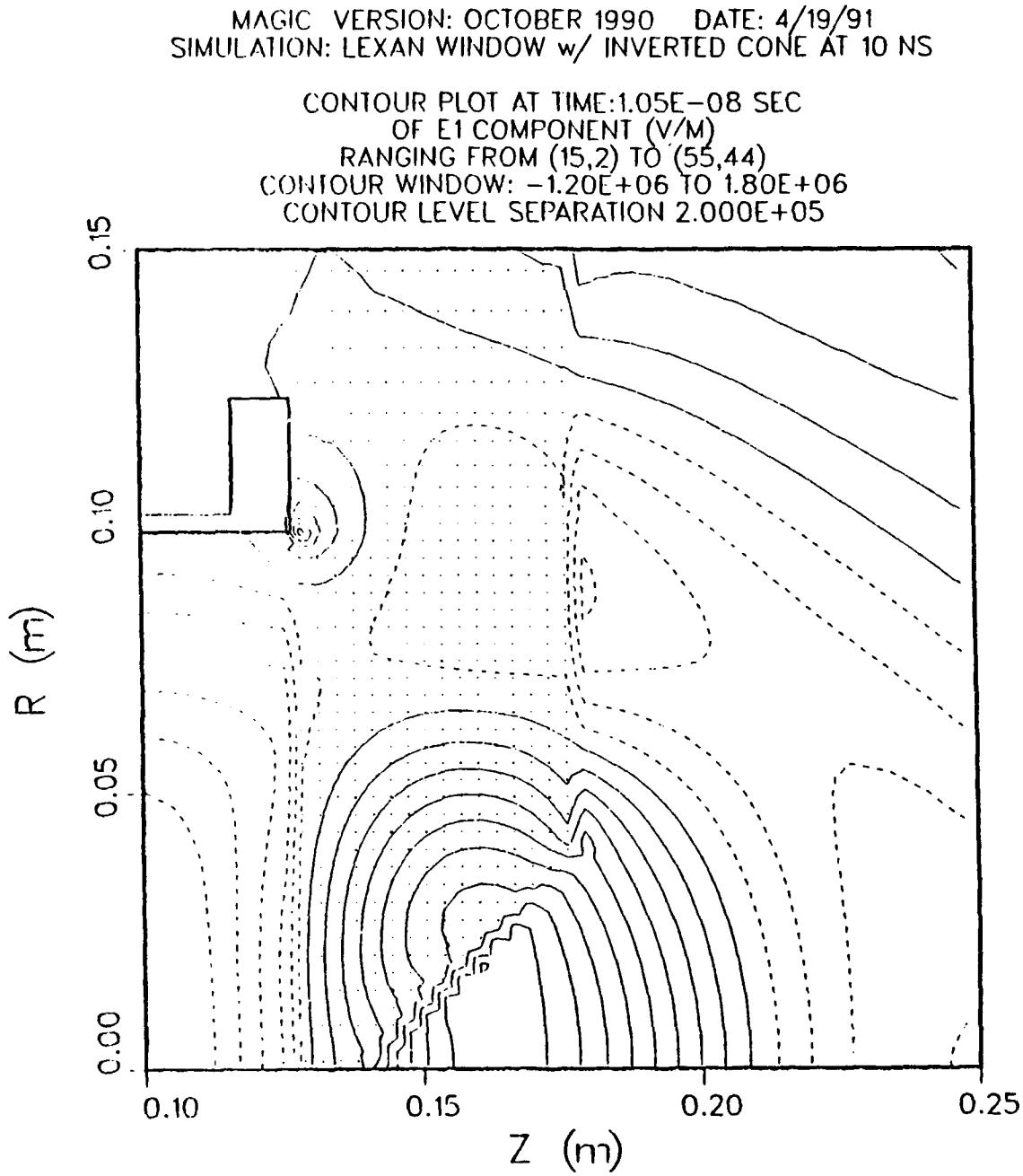

Figure 20. Axial electric field contours for the inverted cone in atmosphere window.

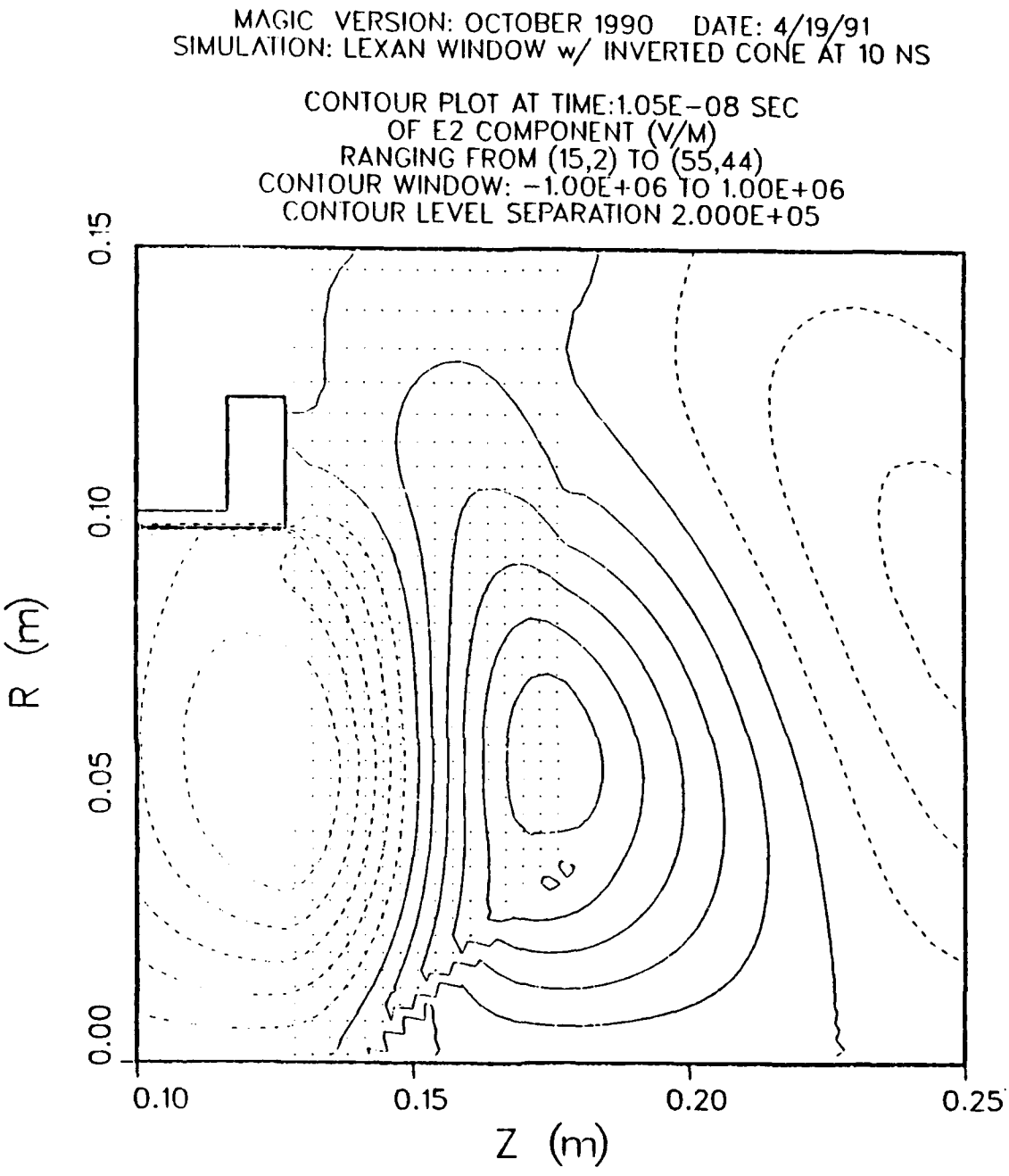

Figure 21. Radial electric field contours for the inverted cone in atmosphere window.

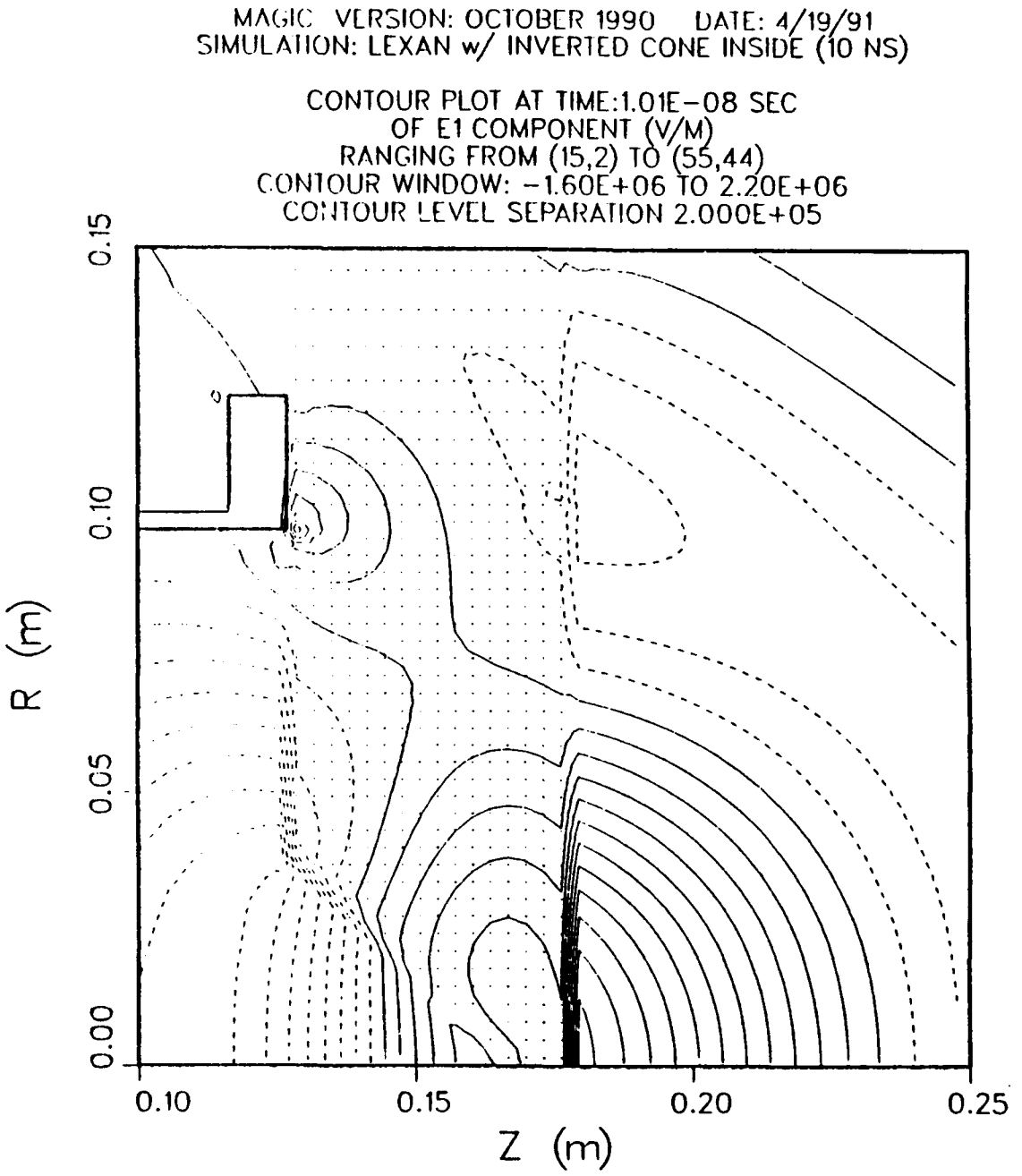

Figure 22. Axial electric field components for the inverted cone in vacuum window.

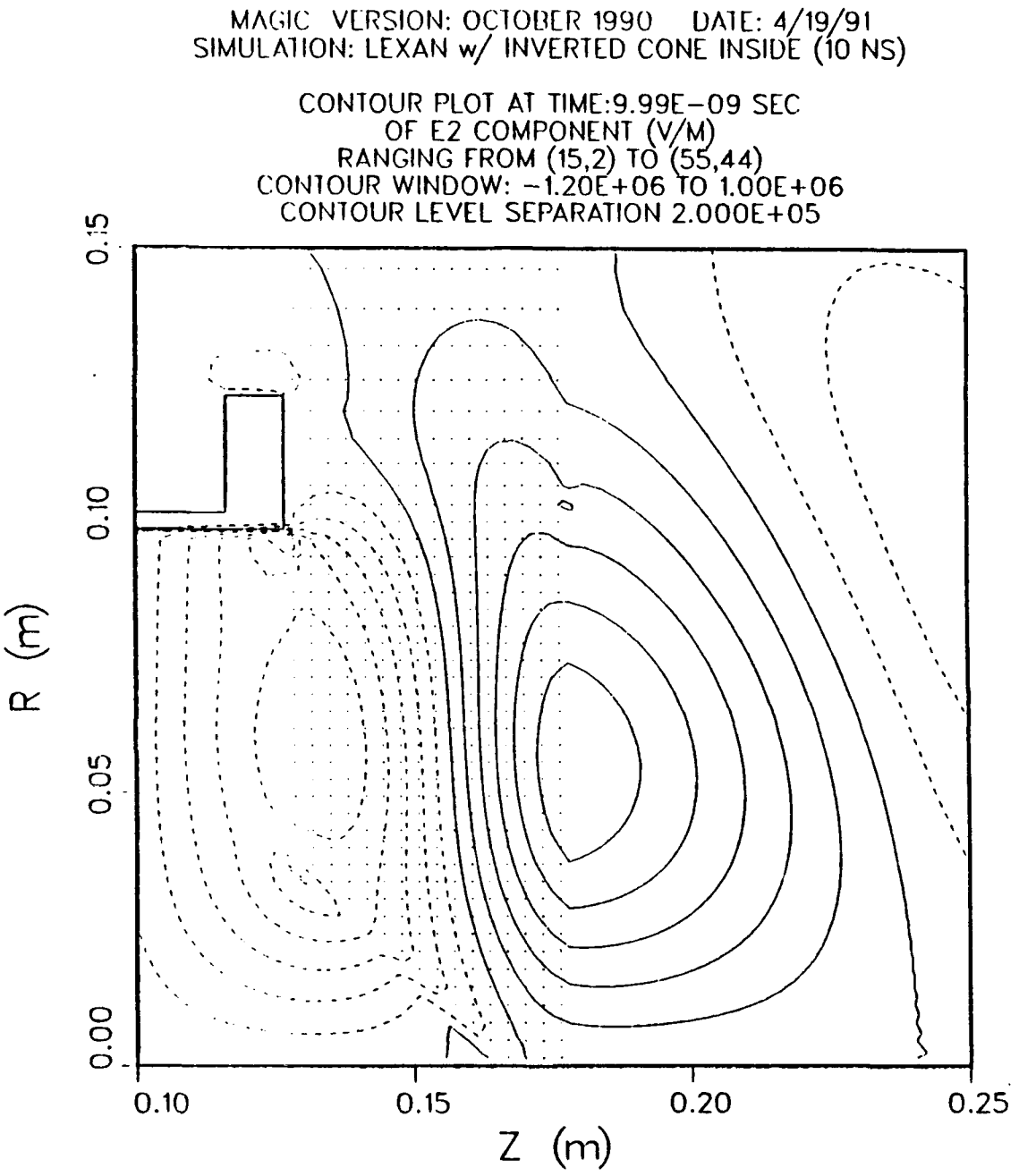

Figure 23. Radial electric field contours for the inverted cone in vacuum window.

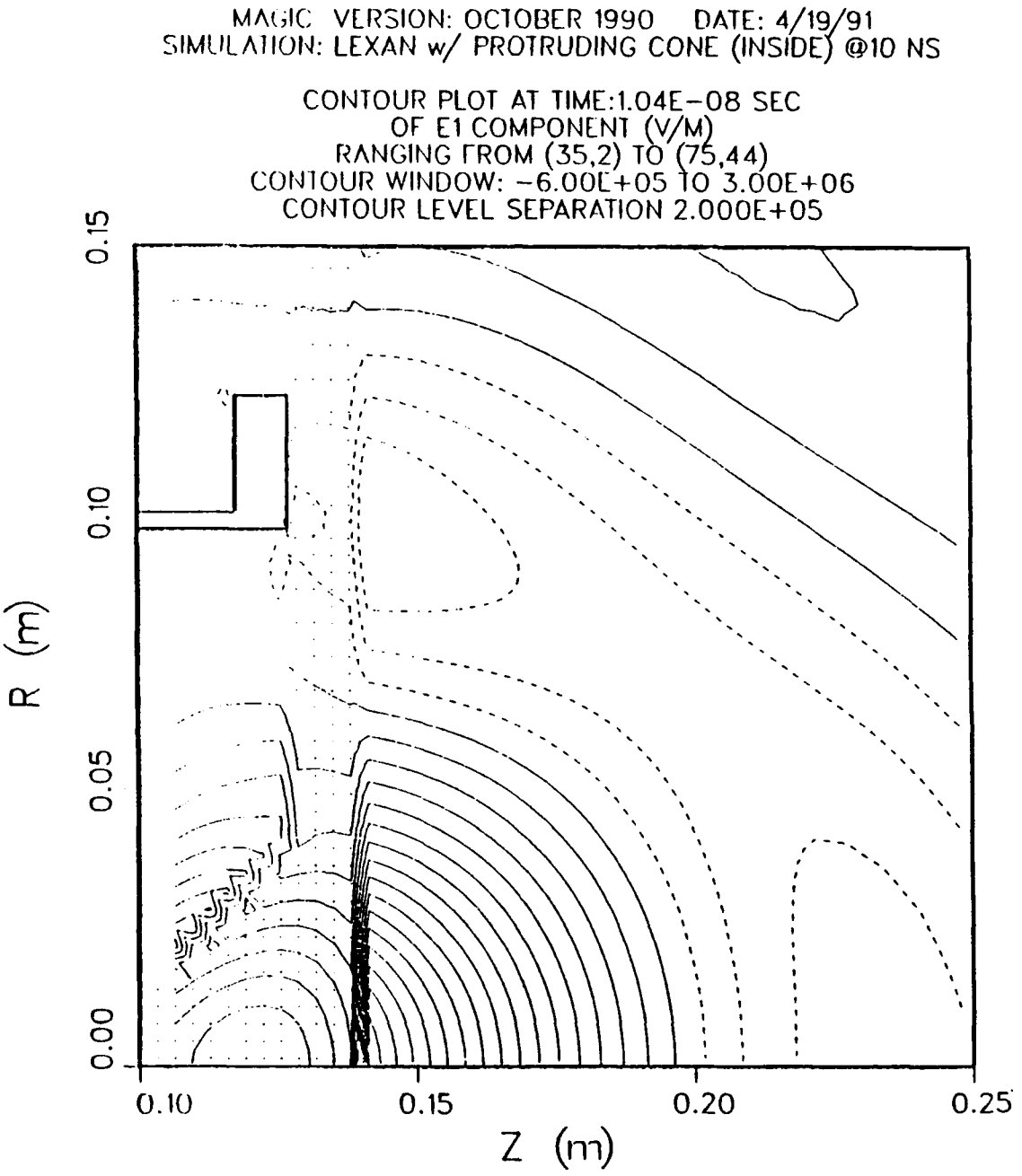

Figure 24. Axial electric field contours for the protruding cone in vacuum window.

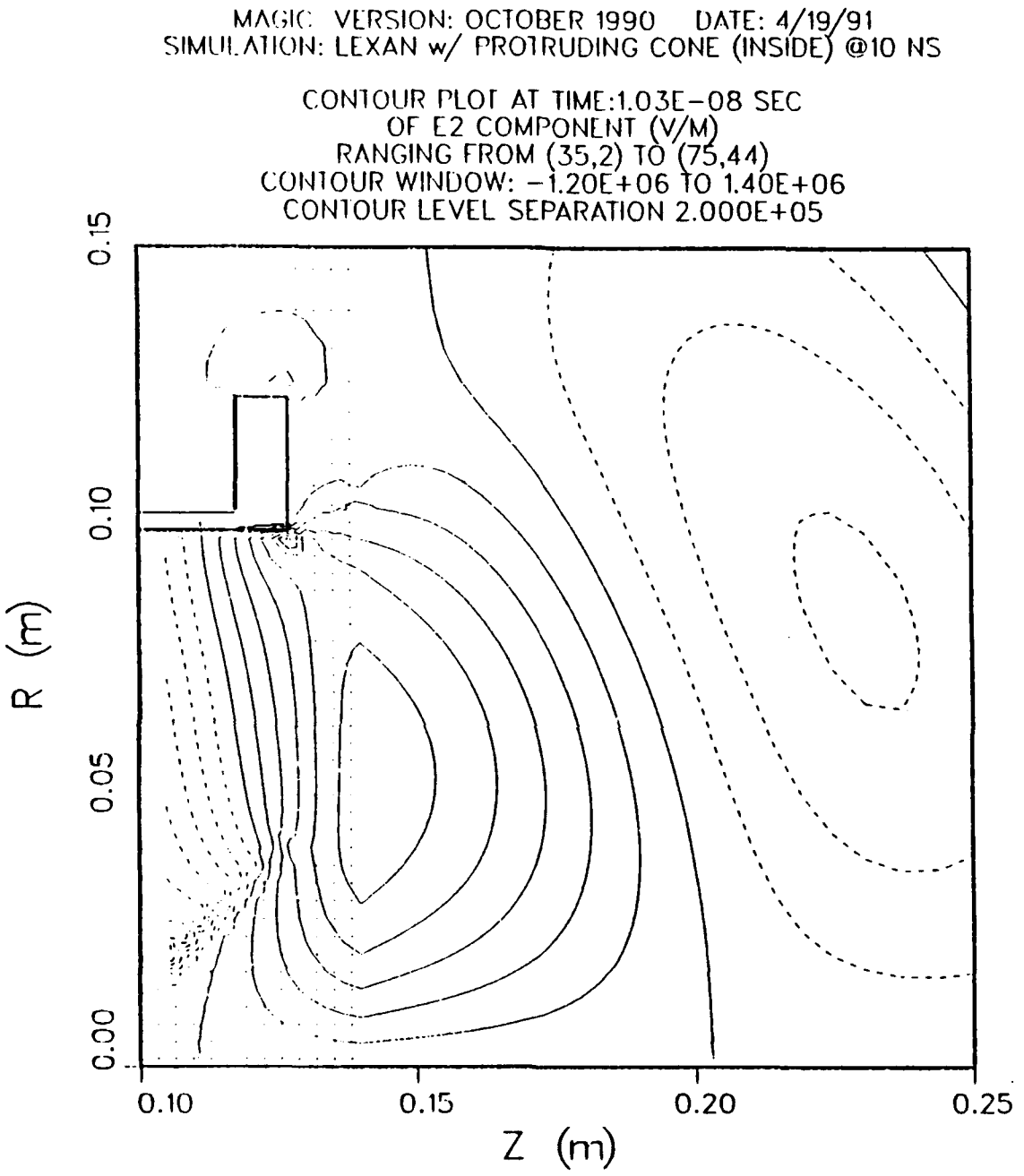

Figure 25. Radial electric field contours for the protruding cone in vacuum window.

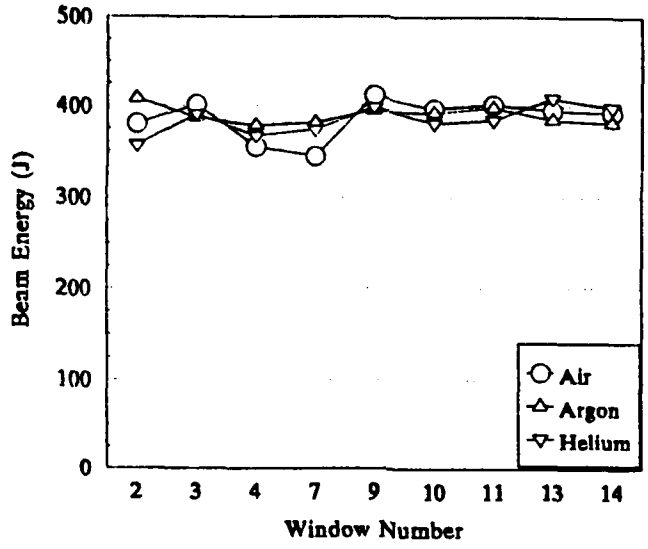

Figure 26. Calculated beam energies for the windows tested.

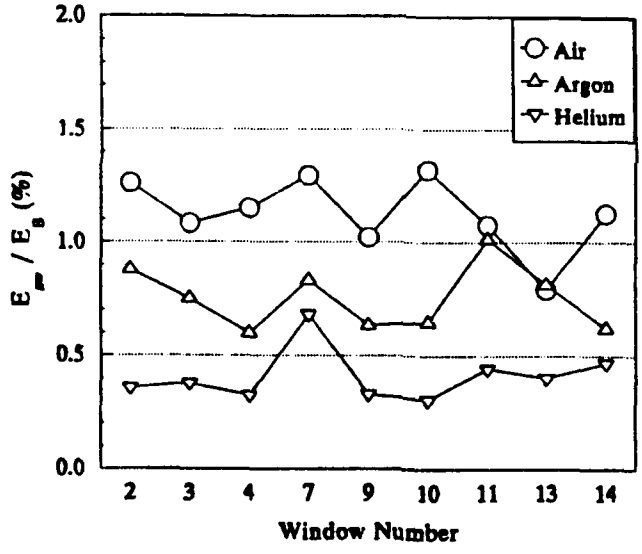

Figure 27. Device efficiencies for the different microwave windows.